

Joint resummation in electroweak boson production

Anna Kulesza^a, George Sterman^b, Werner Vogelsang^c

^a*Department of Physics, Brookhaven National Laboratory, Upton, NY 11973, U.S.A.*

^b*C.N. Yang Institute for Theoretical Physics, SUNY Stony Brook
Stony Brook, New York 11794 – 3840, U.S.A.*

^c*RIKEN-BNL Research Center and Nuclear Theory,
Brookhaven National Laboratory, Upton, NY 11973, U.S.A.*

Abstract

We present a phenomenological application of the joint resummation formalism to electroweak annihilation processes at measured boson momentum Q_T . This formalism simultaneously resums at next-to-leading logarithmic accuracy large threshold and recoil corrections to partonic scattering. We invert the impact parameter transform using a previously described analytic continuation procedure. This leads to a well-defined, resummed perturbative cross section for all nonzero Q_T , which can be compared to resummation carried out directly in Q_T space. From the structure of the resummed expressions, we also determine the form of nonperturbative corrections to the cross section and implement these into our analysis. We obtain a good description of the transverse momentum distribution of Z bosons produced at the Tevatron collider.

1. Introduction

The hadronic annihilation cross sections for electroweak boson production (γ^* , W, Z, H) provide important test cases for resummation techniques in QCD. This paper describes the application of a simultaneous, joint resummation of threshold and transverse momentum singularities in these cross sections. The application to this well-studied case enables us to compare joint resummation to the data for Z production at the Tevatron. We regard it as a first step toward extending joint resummation to a wider range in kinematics and reactions, and toward a unified description of nonperturbative contributions in hadronic reactions.

At measured transverse momentum $Q_T \ll Q$, with Q the pair or boson mass, annihilation cross sections have contributions $\alpha_s^n \ln^{2n-1}(Q_T^2/Q^2)/Q_T^2$ at each order of perturbation theory. Although highly singular at $Q_T = 0$, these terms nevertheless organize themselves into a function that describes the Sudakov suppression of the cross section at small Q_T [1, 2, 3, 4]. These singularities reflect the recoil of the produced electroweak boson against soft gluon radiation. This is transverse momentum resummation, or “ Q_T ” resummation, for short.

Perturbative corrections in factorized inclusive electroweak annihilation cross sections,

$$\frac{d\sigma_{AB}^{\text{res}}}{dQ^2} = \int dz \int dx_i dx_j f_{i/A}(x_i, \mu_F) f_{j/B}(x_j, \mu_F) \delta(z - Q^2/x_i x_j S) \omega_{ij}^{\text{res}}(z, Q, \mu, \mu_F), \quad (1)$$

have an analogous behavior at $z = 1$. In this expression, the f 's are parton distribution functions in hadrons A and B , with ω_{ij}^{res} the corresponding partonic hard-scattering functions, μ is the renormalization scale and μ_F the factorization scale. At $z = 1$, referred to as partonic threshold, $\omega_{ij}^{\text{res}}(z)$ has terms of the form $\alpha_s^n \ln^{2n-1}(1-z)/(1-z)$. These singular corrections reflect the lack of phase space for soft radiation when the partons have just enough energy to produce the observed final state. Like singularities at $Q_T = 0$, they can be resummed to all orders [5, 6].

Unlike transverse momentum resummation, the singular functions of threshold resummation do not appear as explicit logarithms in the physical cross section, Eq. (1), since they are in convolution with the parton distribution functions. In practice, transverse momentum resummation is usually of greater numerical significance at measured Q_T than is threshold resummation at integrated Q_T , simply because the typical value of z in Eq. (1) is generally far from unity. In such cases, threshold resummation shows that the effects of distributions singular at $z = 1$ are under control. It also leads to cross sections that are in general less sensitive to the factorization scale [7]. For this reason, and because the dynamical origins of the large corrections in both threshold and transverse momentum resummations are in soft gluon emission, it is attractive to develop a formalism that encompasses both. The necessary analysis for this combination, which we refer to as joint resummation, has been carried out in [8] for parton distributions, and in [9] for electroweak annihilation as well as QCD cross sections. The effects of resummation are closely bound to momentum conservation. The singular corrections associated with soft gluon emission exponentiate in the corresponding spaces of moments, impact parameter for transverse momentum, and Mellin (or Laplace) moments in energy for threshold resummation. The transforms relax momentum and energy conservation, while their inverses reimpose it. In joint resummation, both transverse momentum and energy conservation are respected.

In Ref. [10], a preliminary analysis of prompt photon production was carried out from the point of view of joint resummation, with an emphasis on the role of recoil in higher-order terms in the relevant hard scattering functions. Relatively substantial effects were found in that case. In this context, it is important to return to the better-understood example of electroweak annihilation to test the joint formalism.

As mentioned above, there is a close relation between resummation and nonperturbative corrections. Taking into account nonleading logarithms and the running of the coupling, resummation leads in each case to a perturbative expression in which the scale of the coupling reflects the value of the transform variable. Because of the singularity of the perturbative effective coupling at Λ_{QCD} , the resulting expressions are, strictly speaking, undefined. A closer look, however, shows that singular contributions appear only at nonleading powers of momentum transfer. This is an example of how perturbative resummation can suggest the way nonperturbative dynamics is expressed in infrared safe hard scattering functions. In effect, perturbation theory is ambiguous, and the resolution of its ambiguities is, by definition, nonperturbative [11, 12]. As we shall review below, these ambiguities manifest themselves as singularities in the integrand of the inverse transforms for both transverse momentum and threshold resummations. Each scheme for dealing with these singularities constitutes a specification of perturbation theory, and implies a parameterization of nonperturbative effects. We hope that a joint resummation affords a more general approach to this problem.

For each resummed cross section, be it Q_T , threshold or joint, one must first specify how to define perturbation theory in the transform space, and then, given a well-defined expression, how to invert the transform. The most “conservative” approach is to expand the resummed expression to some fixed order in perturbation theory [13]. Since the resummation contains information on singular terms at all orders, we may in this way get information beyond the order at which a complete calculation has been done. To fixed order, the perturbative expression and its transform are unambiguous. This approach is applicable to threshold resummation for inclusive cross sections, but is not directly useful for phenomenology at measured $Q_T \sim 0$, where the cross section is singular. Another approach for Q_T resummation is to use the exponentiation of leading logarithms in transverse momentum space, and incorporate the finite order improvements, including those due to the running coupling and momentum conservation, by a direct expansion [14, 15]. A similar application for threshold resummation was developed in [16].

Finally, in both Q_T and threshold resummation, we may, as indicated above, redefine the resummed perturbation theory in transform space, and invert the resulting transform numerically. For threshold resummation this has been done by so-called principal-value [11, 17] and minimal [18] prescriptions for perturbation theory. Both exploit the analytic structure of the running coupling, and redefine transform integrals to avoid the Landau pole. For Q_T resummation, the commonly-used approach (the b_* -prescription) [4, 19, 20, 21, 22] introduces an infrared scale, beyond which the running of the coupling is decoupled from the transform variable. More recently, Qiu and Zhang [23] have proposed another method, employing a smooth extrapolation of the perturbative resummed cross section in impact parameter space to push the Landau singularity to infinity.

In this paper, we will study the jointly resummed cross section derived in [9], defined by a next-to-leading logarithm approximation to the resummed exponent, and an analytic continuation of the b -space contour following [10]. We stress that we could have made other choices, like those mentioned above, within the context of joint resummation. We find the approach of [10], reviewed below, attractive for its simplicity. It results in a redefined perturbative series with no new dimensional scale beyond Λ_{QCD} . Phenomenological parameters then appear only as nonperturbative power corrections. In this “test case” for joint resummation, we shall find a consistency with the data from Z production that we believe is comparable to that of other approaches. We hope that this will serve as a starting-point for further development.

We note that different treatments of the perturbative exponent may differ markedly in pure

threshold resummation, due to different treatments of nonleading logarithms [17, 18, 24]. This important question applies to joint resummation as well, but we shall not explore these differences in this paper. This is because the vector boson cross sections discussed here are in the kinematic region described above, where z is far from unity in Eq. (1), and where we expect the effect of pure threshold resummation to be small in any scheme.

We begin our technical discussion with a review of the joint resummation formalism of Ref. [9], applied to Z production, including a comparison to the exact $\mathcal{O}(\alpha_s)$ cross section. We develop the phenomenological evaluation of the resulting expressions in Sec. 3. This includes the specification of resummed perturbation theory through contour integrals in the two transform spaces, the matching to finite order calculations, and the parameterization of nonperturbative effects. In Sec. 4, we compare the resulting expressions to CDF and D0 data, fitting the necessary nonperturbative parameter. Following this, we give a few preliminary conclusions on the status and prospects of the joint resummation program. In Appendix A, we present some well-known formulas that are relevant for our calculation, and in Appendix B, we sketch the simple numerical method that enables us to evaluate resummed moment space integrals for parton distribution functions that are specified only in x -space.

2. The jointly resummed cross section

Within the formalism of [9], the jointly resummed cross section $d\sigma^{\text{res}}/dQ^2 dQ_T^2$ for electroweak annihilation is obtained as a double inverse Mellin and Fourier (impact parameter) transform:

$$\begin{aligned} \frac{d\sigma_{AB}^{\text{res}}}{dQ^2 dQ_T^2} &= \sum_a \sigma_a^{(0)} \int_{C_N} \frac{dN}{2\pi i} \tau^{-N} \int \frac{d^2b}{(2\pi)^2} e^{i\vec{Q}_T \cdot \vec{b}} \\ &\times \mathcal{C}_{a/A}(Q, b, N, \mu, \mu_F) \exp \left[E_{a\bar{a}}^{\text{PT}}(N, b, Q, \mu) \right] \mathcal{C}_{\bar{a}/B}(Q, b, N, \mu, \mu_F). \end{aligned} \quad (2)$$

Here, $\tau = Q^2/S$, and $\sigma_a^{(0)}$ is a normalization containing the appropriate electroweak charges occurring in the basic underlying process $a\bar{a} \rightarrow V$. For completeness, and because this is the process we will study numerically in this paper, we give $\sigma_a^{(0)}$ for Z production in Appendix A.

Compared to the expression given in [9], we have brought the cross section into a form that is closer to the standard one [4] in Q_T resummation. Resummation of soft-gluon effects is achieved through the flavor-diagonal Sudakov exponent $E_{a\bar{a}}^{\text{PT}}(N, b, Q, \mu)$, while the “ \mathcal{C} -coefficients” contain the parton distribution functions and provide resummation of additional logarithms of soft-collinear and collinear origin. We will discuss the various terms in turn.

2.1. The Sudakov exponent

We now develop an expression for the exponent $E_{a\bar{a}}^{\text{PT}}$, valid to next-to-leading logarithms (NLL) in N and b , based on the results of Ref. [9]. Compared to that reference, we will absorb some terms in the exponent that are associated with parton evolution into the \mathcal{C} -coefficients. We begin with the exponent derived in [9] for the eikonal approximation to $a\bar{a}$ annihilation to an electroweak boson, $E_{a\bar{a}}^{\text{eik}}$. It is given by:

$$E_{a\bar{a}}^{\text{eik}}(N, b, Q, \mu, \mu_F) = 2 \int_0^{Q^2} \frac{dk_T^2}{k_T^2} A_a(\alpha_s(k_T)) \left[J_0(bk_T) K_0 \left(\frac{2Nk_T}{Q} \right) + \ln \left(\frac{\bar{N}k_T}{Q} \right) \right]$$

$$-2 \ln(\bar{N}) \int_{\mu_F^2}^{Q^2} \frac{dk_T^2}{k_T^2} A_a(\alpha_s(k_T)) . \quad (3)$$

Here, J_0 and K_0 are the usual Bessel functions, and we define

$$\bar{N} = N e^{\gamma_E} , \quad (4)$$

with γ_E the Euler constant. The function $A_a(\alpha_s)$ is a series in α_s ,

$$A_a(\alpha_s) = \frac{\alpha_s}{\pi} A_a^{(1)} + \left(\frac{\alpha_s}{\pi}\right)^2 A_a^{(2)} + \dots , \quad (5)$$

in terms the familiar coefficients [25]:

$$\begin{aligned} A_a^{(1)} &= C_a \quad (C_q = C_F, C_g = C_A) , \\ A_a^{(2)} &= \frac{C_a}{2} K \quad , \quad K = C_A \left(\frac{67}{18} - \frac{\pi^2}{6} \right) - \frac{10}{9} T_R N_F . \end{aligned} \quad (6)$$

Dependence on the renormalization scale is implicit in Eq. (3) through the expansion of $\alpha_s(k_T)$ in powers of $\alpha_s(\mu)$.

Following Refs. [9, 4, 26], we approximate the exponent in Eq. (3) by a “minimal” form that is accurate to next-to-leading logarithm in both transform variables:

$$E_{a\bar{a}}^{\text{eik}}(N, b, Q, \mu, \mu_F) = 2 \int_{Q^2/\chi^2}^{Q^2} \frac{dk_T^2}{k_T^2} A_a(\alpha_s(k_T)) \ln\left(\frac{\bar{N} k_T}{Q}\right) - 2 \ln(\bar{N}) \int_{\mu_F^2}^{Q^2} \frac{dk_T^2}{k_T^2} A_a(\alpha_s(k_T)) . \quad (7)$$

Here, the function $\chi(\bar{N}, \bar{b})$ organizes the logarithms of N and b in joint resummation,

$$\chi(\bar{N}, \bar{b}) = \bar{b} + \frac{\bar{N}}{1 + \eta \bar{b}/\bar{N}} , \quad (8)$$

where η is a constant, and where, by analogy to \bar{N} of Eq. (4), we have defined

$$\bar{b} \equiv b Q e^{\gamma_E} / 2 . \quad (9)$$

To anticipate, we will choose $\eta = 1/4$ below. We will discuss the particular expression (8) for χ in the next subsection.

We now regroup Eq. (7) as

$$E_{a\bar{a}}^{\text{eik}}(N, b, Q, \mu, \mu_F) = 2 \int_{Q^2/\chi^2}^{Q^2} \frac{dk_T^2}{k_T^2} A_a(\alpha_s(k_T)) \ln\left(\frac{k_T}{Q}\right) - 2 \ln(\bar{N}) \int_{\mu_F^2}^{Q^2/\chi^2} \frac{dk_T^2}{k_T^2} A_a(\alpha_s(k_T)) . \quad (10)$$

Next, we make contact with standard Q_T resummation by writing

$$\begin{aligned} E_{a\bar{a}}^{\text{eik}}(N, b, Q, \mu, \mu_F) &= - \int_{Q^2/\chi^2}^{Q^2} \frac{dk_T^2}{k_T^2} \left[A_a(\alpha_s(k_T)) \ln\left(\frac{Q^2}{k_T^2}\right) + B_a(\alpha_s(k_T)) \right] \\ &+ \int_{\mu_F^2}^{Q^2/\chi^2} \frac{dk_T^2}{k_T^2} \left[-2A_a(\alpha_s(k_T)) \ln(\bar{N}) - B_a(\alpha_s(k_T)) \right] . \end{aligned} \quad (11)$$

Here we have introduced

$$B_a(\alpha_s) = \frac{\alpha_s}{\pi} B_a^{(1)} + \left(\frac{\alpha_s}{\pi}\right)^2 B_a^{(2)} + \dots, \quad (12)$$

with

$$B_q^{(1)} = -\frac{3}{2}C_F, \quad B_g^{(1)} = -\frac{1}{6}(11C_A - 4T_R N_F). \quad (13)$$

Eq. (11) follows from Eq. (10) to NLL accuracy in N and b . The coefficients $B_a^{(2)}$ are also known [19, 27], but contribute only beyond NLL.

The first term in Eq. (11),

$$- \int_{Q^2/\chi^2}^{Q^2} \frac{dk_T^2}{k_T^2} \left[A_a(\alpha_s(k_T)) \ln\left(\frac{Q^2}{k_T^2}\right) + B_a(\alpha_s(k_T)) \right], \quad (14)$$

has the classic form of the Sudakov exponent in electroweak annihilation, the only new ingredient being the quantity χ that depends on N and b and represents the joint resummation. As shown in Sec. 3.1 of Ref. [9], the term with B_a accounts for the difference between the eikonal approximation and the full partonic cross sections in the threshold region. Eq. (14) will be our choice for the exponent $E_{a\bar{a}}^{\text{PT}}$ in Eq. (2). Its expansion in leading and next-to-leading logarithms gives

$$E_{a\bar{a}}^{\text{PT}}(N, b, Q, \mu) = \frac{2}{\alpha_s(\mu)} h_a^{(0)}(\beta) + 2h_a^{(1)}(\beta, Q, \mu), \quad (15)$$

where

$$h_a^{(0)}(\beta) = \frac{A_a^{(1)}}{2\pi b_0^2} [2\beta + \ln(1 - 2\beta)], \quad (16)$$

$$\begin{aligned} h_a^{(1)}(\beta, Q, \mu) &= \frac{A_a^{(1)} b_1}{2\pi b_0^3} \left[\frac{1}{2} \ln^2(1 - 2\beta) + \frac{2\beta + \ln(1 - 2\beta)}{1 - 2\beta} \right] + \frac{B_a^{(1)}}{2\pi b_0} \ln(1 - 2\beta) \\ &+ \frac{1}{2\pi b_0} \left[A_a^{(1)} \ln\left(\frac{Q^2}{\mu^2}\right) - \frac{A_a^{(2)}}{\pi b_0} \right] \left[\frac{2\beta}{1 - 2\beta} + \ln(1 - 2\beta) \right]. \end{aligned} \quad (17)$$

In these equations,

$$\begin{aligned} \lambda &= b_0 \alpha_s(\mu) \ln(\bar{N}), \\ \beta &= b_0 \alpha_s(\mu) \ln(\chi), \end{aligned} \quad (18)$$

and

$$b_0 = \frac{11C_A - 4T_R N_F}{12\pi}, \quad b_1 = \frac{17C_A^2 - 10C_A T_R N_F - 6C_F T_R N_F}{24\pi^2}. \quad (19)$$

In order to interpret the second term in Eq. (11), we note that the combination in its square brackets,

$$-2A_a(\alpha_s) \ln(\bar{N}) - B_a(\alpha_s), \quad (20)$$

corresponds to the leading (logarithmic plus constant) terms at large N in the one-loop diagonal $q \rightarrow q$ (or, $g \rightarrow g$) anomalous dimension. To be more precise, the way we have obtained

Eq. (11), the second term in Eq. (11) matches the anomalous dimension to NLL accuracy only, since the constant (in N) part of the two-loop anomalous dimension is not identical to the customary [19, 20, 21, 22] coefficient $B_a^{(2)}$ (even though it is related to it [27, 28]). As mentioned above, contributions related to $B_a^{(2)}$ enter only beyond NLL and are outside the presently developed reach of the joint resummation formalism. We are therefore indeed free to associate the combination in Eq. (20) with the leading terms in the anomalous dimension. It then follows that the second term in Eq. (11) represents the evolution of the parton densities from scale μ_F to scale Q/χ in the large- N limit, that is, near threshold. Note that indeed all dependence of the exponent $E_{a\bar{a}}^{\text{eik}}$ on μ_F is contained in this term. The evolution term we have identified in Eq. (11) will become part of the functions $\mathcal{C}_{a/H}$ introduced in Eq. (2). We shall therefore pursue it further when discussing the $\mathcal{C}_{a/H}$ in subsection 2.3. below.

2.2. The function $\chi(\bar{N}, \bar{b})$

We have defined $\chi(\bar{N}, \bar{b})$ in Eq. (8). There is an element of choice in the actual form of $\chi(\bar{N}, \bar{b})$, the only requirement being that the leading and next-to-leading logarithms of \bar{N} and \bar{b} are correctly reproduced in the limits $\bar{N} \rightarrow \infty$ or $\bar{b} \rightarrow \infty$, respectively. In ref. [9], the somewhat simpler choice

$$\chi(\text{Ref. [9]}) = \bar{b} + \bar{N} \quad (21)$$

was made. While this is a legitimate option, we found it to be less convenient for phenomenological studies. The reason for this is that this form of χ introduces sizable subleading terms into perturbative expansions of the resummed exponent, which are not present in full fixed-order perturbative results. For instance, expanding the exponent $E_{a\bar{a}}^{\text{PT}}(N, b, Q, \mu)$ in Eq. (15) to $\mathcal{O}(\alpha_s(\mu))$ one finds:

$$\exp \left[E_{a\bar{a}}^{\text{PT}}(N, b, Q, \mu) \right] \approx 1 - \frac{2\alpha_s(\mu)}{\pi} C_F \left[\ln^2(\chi) - \frac{3}{2} \ln(\chi) \right]. \quad (22)$$

If we are assuming that $\bar{b} \gg \bar{N}$, relevant at small Q_T far away from threshold, then this is approximately

$$\exp \left[E_{a\bar{a}}^{\text{PT}}(N, b, Q, \mu) \right] \approx 1 - \frac{2\alpha_s(\mu)}{\pi} C_F \left[\ln^2(\bar{b}) - \frac{3}{2} \ln(\bar{b}) + 2\frac{\bar{N}}{\bar{b}} \ln(\bar{b}) + \mathcal{O}\left(\frac{1}{\bar{b}}\right) \right]. \quad (23)$$

On the other hand, the fixed order $\mathcal{O}(\alpha_s)$ result for the partonic cross section for flavor a is given (at $Q_T \neq 0$) by [2]:

$$\frac{d\hat{\sigma}^{\mathcal{O}(\alpha_s)}}{dQ^2 dQ_T^2} = \sigma_a^{(0)} \frac{\alpha_s(\mu)}{\pi} C_F \left[\frac{\ln(Q^2/Q_T^2)}{Q_T^2} - \frac{3}{2Q_T^2} + \mathcal{O}\left(\ln(Q^2/Q_T^2)\right) \right], \quad (24)$$

where we have indicated the functional form of the first Q_T -suppressed correction. It is easy to show that upon Fourier transformation of the $\mathcal{O}(\alpha_s)$ in Eq. (23) back to Q_T space, the first two terms $\ln^2(\bar{b}) - \frac{3}{2} \ln(\bar{b})$ reproduce the first two contributions to $d\hat{\sigma}/dQ^2 dQ_T^2$ in Eq. (24). The term $\propto \ln(\bar{b})/\bar{b}$ in Eq. (23), however, yields a subleading contribution to the cross section, which is of the form $\ln(Q_T^2/Q^2)/Q_T$, that is, down with respect to the leading and next-to-leading logarithms, but more singular than the first suppressed correction to the fixed order cross section in Eq. (24) which is just $\propto \ln(Q_T^2/Q^2)$. In other words, the choice (21) introduces new dependence of the resummed cross section on Q_T , not present in the cross section calculated at fixed order.

Even though this affects only subleading, integrable terms, which are beyond the reach of our resummation anyway, this mismatch between Eqs. (22) and (24) at $\mathcal{O}(1/Q_T)$ produces a spurious logarithmic singularity in $d\sigma/dQ^2 dQ_T$, which is the cross section we will compare to the data. This problem is avoided to all orders by choosing χ as in Eq. (8) with any $\eta > 0$.

The function χ in Eq. (8) is only a slight modification of Eq. (21), but it has the property that at large \bar{b} corrections to the leading term are suppressed as $1/\bar{b}^2$. In this way, no dependence of the form $\ln(Q_T^2/Q^2)/Q_T$ can arise in the cross section in Q_T space. Obviously, the general limits for $\bar{b} \rightarrow \infty$ and $\bar{N} \rightarrow \infty$ are the same as in (21). It also turns out that this form of $\chi(\bar{N}, \bar{b})$ leads to analytic properties of the exponent in Eq. (15) that are consistent with the method described below for performing the inverse transform in b .

We will analyze expansions of our final resummed cross section to one loop in more detail in subsec. 2.4.. Before doing so, we need to specify the coefficients $\mathcal{C}_{a/H}(Q, b, N, \mu, \mu_F)$ of Eq. (2).

2.3. The coefficients $\mathcal{C}_{a/H}(Q, b, N, \mu, \mu_F)$

The coefficients $\mathcal{C}_{a/H}(Q, b, N, \mu, \mu_F)$ in Eq. (2) are chosen to correspond to the jointly resummed cross section in [10] for large N and arbitrary b , and to Q_T resummation for $b \rightarrow \infty$, N fixed:

$$\mathcal{C}_{a/H}(Q, b, N, \mu, \mu_F) = \sum_{j,k} C_{a/j}(N, \alpha_s(\mu)) \mathcal{E}_{jk}(N, Q/\chi, \mu_F) f_{k/H}(N, \mu_F). \quad (25)$$

Here the $f_{j/H}(N, \mu_F)$ are again the parton distribution functions for hadron H at factorization scale μ_F . In principle, by analogy with standard Q_T resummation [4], the scale for the strong coupling in the $C_{a/j}(N, \alpha)$ would be Q/χ ; however, at the NLL level we are considering here, it is legitimate to choose the ‘‘large’’ renormalization scale $\mu \sim Q$ and to expand the $C_{a/j}(N, \alpha)$ to a finite order in α_s . To first order, matching Eq. (25) to the large- b behavior of the Q_T -resummed cross section [2, 4, 19, 28], one has

$$C_{q/q}(N, \alpha_s) = 1 + \frac{\alpha_s}{4\pi} C_F \left(-8 + \pi^2 + \frac{2}{N(N+1)} \right) = C_{\bar{q}/\bar{q}}(N, \alpha_s), \quad (26)$$

$$C_{q/g}(N, \alpha_s) = \frac{\alpha_s}{2\pi} \frac{1}{(N+1)(N+2)} = C_{\bar{q}/g}(N, \alpha_s). \quad (27)$$

Note that the coefficient $C_{q/g}$ is off-diagonal in flavor. It is indeed a well-known feature in Q_T resummation [4, 19, 2, 28] that such non-diagonal terms also contribute to singular behavior at $Q_T = 0$. On the other hand, they do not incorporate singularities at threshold, which is visible from the fact that $C_{q/g}$ is suppressed at large N .

The evolution matrix $\mathcal{E}(N, Q/\chi, \mu_F)$ in Eq. (25) results from the second term in Eq. (11) that we chose to absorb into the \mathcal{C} coefficients. Compared to the large- N limit used in that equation and relevant near threshold, we can make an improvement here and replace the leading- N part of the diagonal anomalous dimension in Eqs. (20) and (11) by the *full* anomalous dimension relevant for the scale evolution of parton densities, containing also all terms subleading in N :

$$-2A_a(\alpha_s) \ln(\bar{N}) - B_a(\alpha_s) \longrightarrow \gamma_N(\alpha_s). \quad (28)$$

At NLL level, where $A_a^{(1)}$, $B_a^{(1)}$, $A_a^{(2)}$ contribute, we need the first two terms in the perturbative expansion of the anomalous dimension [29], $\gamma_N = \frac{\alpha_s}{\pi} \gamma_N^{(0)} + \left(\frac{\alpha_s}{\pi}\right)^2 \gamma_N^{(1)}$. Since the $\gamma_N^{(i)}$ are (in

general) matrices, this procedure introduces terms that are parton non-diagonal, and thus leads to the matrix structure of \mathcal{E} in terms of an ordered exponential. As mentioned above, the interpretation of \mathcal{E} is simply the evolution of the parton densities from scale μ_F to scale Q/χ , within the NLL approximation. In this way, it leads to a resummation of collinear logarithms, some of which are associated with partonic threshold, that is, are also proportional to $\ln \bar{N}$, while others are suppressed by $\mathcal{O}(1/N)$ or more, due to partonic mixing. Such a procedure is also familiar from standard Q_T resummation [4, 28], and the substitution in Eq. (28) thus provides a natural extension of our formalism for joint resummation away from threshold. We may also interpret $\mathcal{C}_{a/H}(Q, b, N, \mu, \mu_F)$ as the Fourier-Mellin transform of a generalized parton distribution, at measured transverse momentum and energy fraction [9]. Eq. (25) then has the interpretation of a refactorization of $\mathcal{C}_{a/H}$ into a coefficient function $C_{a/j}$ and light cone parton distribution functions, $f_{j/H}$, at the scale Q/χ .

Explicit expressions for the solution of the standard evolution equations for parton densities between scales μ_F and Q/χ can be found in [30, 31] and can be used to determine the elements of the matrix \mathcal{E} . To achieve the exponentiation of the evolution terms – despite the fact that the matrices $\gamma_N^{(0)}$ and $\gamma_N^{(1)}$ do not commute – the iterative procedure derived in Ref. [31] is particularly useful. The parameter that governs the evolution between scales μ_F and Q/χ is

$$\ln \left(\frac{\alpha_s(\mu_F)}{\alpha_s(Q/\chi)} \right) = \ln(1 - 2\beta) + \alpha_s(\mu) \left[\frac{b_1 \ln(1 - 2\beta)}{b_0 (1 - 2\beta)} + b_0 \ln \left(\frac{Q^2}{\mu^2} \right) \frac{2\beta}{1 - 2\beta} + b_0 \ln \left(\frac{Q^2}{\mu_F^2} \right) \right], \quad (29)$$

where the right-hand-side is the expansion to NLL accuracy, consistent with our approximation. It should be emphasized that in the above expression the scale μ_F appears through a single explicit logarithm that will serve to approximately cancel the μ_F dependence of the parton distributions in Eq. (25), resulting in a decrease in μ_F -dependence for the final resummed cross section in Eq. (2), as compared to a fixed-order calculation.

In all of these procedures, working in Mellin- N moment space is a great convenience, because it enables us to explicitly express the evolution between the scales μ_F and Q/χ in terms of the parameter $\ln(\alpha_s(\mu_F)/\alpha_s(Q/\chi))$ in Eq. (29). In this way, we avoid the problem normally faced in Q_T resummation that one needs to call the parton densities at scales far below their range of validity, so that some sort of “freezing” (or related prescription) for handling the parton distributions is required. As is evident from Eq. (25), we only need the parton distribution functions at the “large” scale $\mu_F \sim Q$, whereas normally in Q_T resummation the product $\sum_k \mathcal{E}_{jk} \left(N, Q/\bar{b}, \mu_F \right) f_{k/H}(N, \mu_F)$ is identified with $f_{k/H}(N, Q/\bar{b})$. An organization of the \mathcal{C} coefficients in a form similar to ours was first proposed in [28]. We finally note that the moment variable N and, as will be discussed below, also the impact parameter b are in general complex-valued in our approach, so that it is even more desirable to separate the complex scale Q/χ from that in the parton densities. In this way, it is not even necessary (albeit convenient) to have the parton densities in Mellin- N moment space, as provided in the code of [32]. In fact, we can generalize our analysis to any set of distribution functions, even if specified only in x space. Details are discussed in Appendix B.

2.4. Finite-order $\mathcal{O}(\alpha_s)$ expansions of the resummed cross section

In this section, we compare expansions of our jointly resummed cross section to “exact” expressions for the electroweak annihilation cross section at $\mathcal{O}(\alpha_s)$. We discuss first the limits

$N \rightarrow \infty$, $b = 0$ and $b \rightarrow \infty$, N fixed separately. In these cases, all results can be given analytically.

The limit $N \rightarrow \infty$, $b = 0$ corresponds to pure threshold resummation for the total cross section. It is realized by integrating over Q_T in Eq. (2), which sets $b = 0$ there. Expansion of Eq. (2) to $\mathcal{O}(\alpha_s)$, using Eqs. (15), (26), (27) and the parton distribution functions evolved according to Eq. (29), then gives for the partonic cross sections in the $q\bar{q}$ and qg scattering channels:

$$\begin{aligned}\hat{\sigma}^{q\bar{q}} &= \sigma_q^{(0)} \frac{\alpha_s}{2\pi} C_F \left\{ -4 \ln^2 \bar{N} + 6 \ln \bar{N} - 8 + \pi^2 + \frac{2}{N(N+1)} \right. \\ &\quad \left. + \left[\frac{2}{N(N+1)} + 3 - 4S_1(N) \right] \left[-2 \ln \bar{N} + \ln \left(\frac{Q^2}{\mu_F^2} \right) \right] \right\} , \\ \hat{\sigma}^{qg} &= \sigma_q^{(0)} \frac{\alpha_s}{2\pi} T_R \left\{ \frac{N^2 + N + 2}{N(N+1)(N+2)} \left[-2 \ln \bar{N} + \ln \left(\frac{Q^2}{\mu_F^2} \right) \right] + \frac{2}{(N+1)(N+2)} \right\} ,\end{aligned}\quad (30)$$

where $S_1(N) = \sum_{j=1}^N j^{-1} = \psi(N+1) + \gamma_E$, with ψ the digamma function. Since we are interested in the near-threshold region, we can expand this further to the large- N limit. Using $\psi(N+1) = \ln N + 1/(2N) + \mathcal{O}(1/N^2)$, we find:

$$\begin{aligned}\hat{\sigma}^{q\bar{q}} &= \sigma_q^{(0)} \frac{\alpha_s}{2\pi} C_F \left\{ 4 \ln^2 \bar{N} + 4 \frac{\ln \bar{N}}{N} - 8 + \pi^2 + \left[3 - \frac{2}{N} - 4 \ln \bar{N} \right] \ln \left(\frac{Q^2}{\mu_F^2} \right) \right\} + \mathcal{O} \left(\frac{\ln \bar{N}}{N^2} \right) , \\ \hat{\sigma}^{qg} &= \sigma_q^{(0)} \frac{\alpha_s}{2\pi} T_R \frac{1}{N} \left[-2 \ln \bar{N} + \ln \left(\frac{Q^2}{\mu_F^2} \right) \right] + \mathcal{O} \left(\frac{\ln \bar{N}}{N^2} \right) .\end{aligned}\quad (31)$$

The Mellin moments of the “exact” $\mathcal{O}(\alpha_s)$ partonic cross sections can be found in [33] and read:

$$\begin{aligned}\hat{\sigma}_{\text{exact}}^{q\bar{q}} &= \sigma_q^{(0)} \frac{\alpha_s}{2\pi} C_F \left\{ 4S_1^2(N) - \frac{4}{N(N+1)} S_1(N) + \frac{2}{N^2} + \frac{2}{(N+1)^2} - 8 + \frac{4\pi^2}{3} \right. \\ &\quad \left. + \left[\frac{2}{N(N+1)} + 3 - 4S_1(N) \right] \ln \left(\frac{Q^2}{\mu_F^2} \right) \right\} , \\ \hat{\sigma}_{\text{exact}}^{qg} &= \sigma_q^{(0)} \frac{\alpha_s}{2\pi} T_R \left\{ -2 \frac{N^2 + N + 2}{N(N+1)(N+2)} S_1(N) + \frac{N^4 + 11N^3 + 22N^2 + 14N + 4}{N^2(N+1)^2(N+2)^2} \right. \\ &\quad \left. + \frac{N^2 + N + 2}{N(N+1)(N+2)} \ln \left(\frac{Q^2}{\mu_F^2} \right) \right\} .\end{aligned}\quad (32)$$

At large N , this gives

$$\begin{aligned}\hat{\sigma}_{\text{exact}}^{q\bar{q}} &= \sigma_q^{(0)} \frac{\alpha_s}{2\pi} C_F \left\{ 4 \ln^2 \bar{N} + 4 \frac{\ln \bar{N}}{N} - 8 + \frac{4}{3} \pi^2 + \left[3 - \frac{2}{N} - 4 \ln \bar{N} \right] \ln \left(\frac{Q^2}{\mu_F^2} \right) \right\} + \mathcal{O} \left(\frac{\ln \bar{N}}{N^2} \right) , \\ \hat{\sigma}_{\text{exact}}^{qg} &= \sigma_q^{(0)} \frac{\alpha_s}{2\pi} T_R \frac{1}{N} \left[-2 \ln \bar{N} + \ln \left(\frac{Q^2}{\mu_F^2} \right) \right] + \mathcal{O} \left(\frac{\ln \bar{N}}{N^2} \right) .\end{aligned}\quad (33)$$

Comparing Eqs. (31) and (33), we see that at large N the expansion of the resummed cross section correctly reproduces the $\mathcal{O}(\alpha_s)$ result, including even all terms that are down by $1/N$. The only difference between (31) and (33) is in the term $\propto \pi^2$. This difference is due to our choice of the coefficient $C_{q/q}$ in Eq. (26), for which we employed a form that is more standard

in Q_T , rather than in threshold, resummation. A closer inspection of our resummed eikonal exponent, Eq. (3), reveals that its Bessel functions result in different contributions $\propto \pi^2$ in the two limits $N \rightarrow \infty$ and $b \rightarrow \infty$, just as needed to explain the deficiency between Eqs. (31) and (33). In other words, we could modify our expansion of the exponent into logarithms somewhat (by suitably redefining χ), so that Eq. (31) would automatically have the correct coefficient of π^2 . On the other hand, the terms associated with π^2 are beyond NLL, which is the scope of the present analysis, and we therefore do not implement this change here.

It is worth pointing out that the reason why we correctly reproduce all terms suppressed as $1/N$ in Eqs. (31) and (33) is our treatment of evolution in Eq. (28). As was discussed in [34], the leading $\ln(\bar{N})/N$ terms are associated with collinear non-soft emission; it is therefore natural that they can be generated from evolution of the parton densities between the scales μ_F and Q/\bar{N} , as embodied in Eq. (29) at $b = 0$. In this way, our joint resummation correctly includes the leading $\alpha_s^k \ln^{2k-1} \bar{N}/N$ terms to all orders. Because threshold resummation has a relatively modest effect for vector boson production in the kinematic region explored at the Tevatron, we leave for future work a more complete comparison of our resummed expression to fixed order, beyond these $\mathcal{O}(\alpha_s)$ considerations.

In the limit $b \rightarrow \infty$, N fixed, our formulas smoothly turn into those for standard Q_T resummation. For the one-loop expansion of the jointly resummed cross section we find

$$\begin{aligned} \hat{\sigma}^{q\bar{q}} &= \sigma_q^{(0)} \frac{\alpha_s}{2\pi} C_F \left\{ -4 \ln^2 \bar{b} + 6 \ln \bar{b} - 8 + \pi^2 + \frac{2}{N(N+1)} \right. \\ &\quad \left. + \left[\frac{2}{N(N+1)} + 3 - 4S_1(N) \right] \left[-2 \ln \bar{b} + \ln \left(\frac{Q^2}{\mu_F^2} \right) \right] \right\} + \mathcal{O}(\ln \bar{b}/b^2) \quad , \\ \hat{\sigma}^{gg} &= \sigma_q^{(0)} \frac{\alpha_s}{2\pi} T_R \left\{ \frac{N^2 + N + 2}{N(N+1)(N+2)} \left[-2 \ln \bar{b} + \ln \left(\frac{Q^2}{\mu_F^2} \right) \right] + \frac{2}{(N+1)(N+2)} \right\} + \mathcal{O}(\ln \bar{b}/b^2) \quad , \end{aligned} \quad (34)$$

in full agreement with the expressions for the large- b limit of the “exact” $\mathcal{O}(\alpha_s)$ result derived in [2].

We do not present closed expressions for arbitrary large N and b , but we can easily compare numerically the exact $\mathcal{O}(\alpha_s)$ result with the expansion of Eq. (2) to $\mathcal{O}(\alpha_s)$. Fig. 1(a) shows the fractional deviation

$$\Delta \equiv \left[\frac{d\sigma^{\text{fixed}(1)}}{dQ_T} - \frac{d\sigma^{\text{exp}(1)}}{dQ_T} \right] / \frac{d\sigma^{\text{fixed}(1)}}{dQ_T} \quad , \quad (35)$$

where $d\sigma^{\text{fixed}(1)}/dQ_T$ is the “exact” $\mathcal{O}(\alpha_s)$ cross section and $d\sigma^{\text{exp}(1)}/dQ_T$ denotes the one-loop expansion of the resummed expression. Fig. 1(b) compares $d\sigma^{\text{fixed}(1)}/dQ_T$ and $d\sigma^{\text{exp}(1)}/dQ_T$ individually. Note the excellent agreement in the region $Q_T < 10$ GeV where resummation is necessary. Beyond 10 GeV, the agreement is naturally less exact but still good. This is the region where matching to finite order is appropriate, to which we will turn now.

3. Inverse transforms and matching

In this section we take the remaining steps necessary to apply the joint resummation formalism phenomenologically. This includes specifying a prescription for performing the inverse integrals in (2), as well as implementing a procedure for matching resummed and finite-order results. In addition, we will consider nonperturbative effects resulting from the strong coupling at small momentum scales.

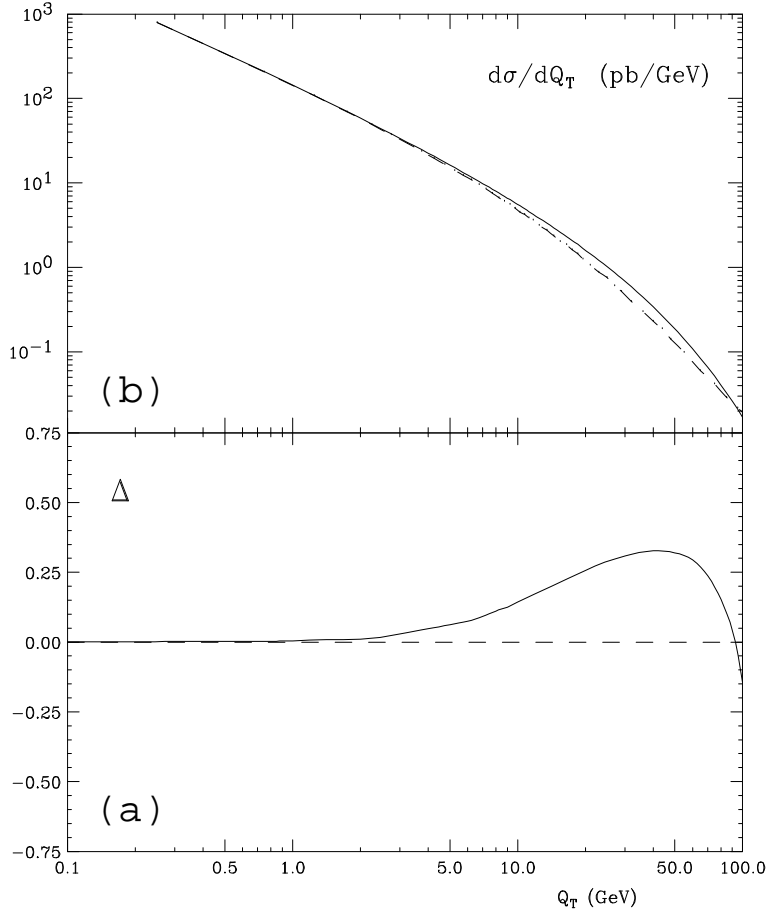


Figure 1: (a) Fractional deviation Δ (as defined in Eq. (35)) between the “exact” $\mathcal{O}(\alpha_s)$ result and the $\mathcal{O}(\alpha_s)$ expansion of the jointly resummed cross section. We consider here Z boson production at the Tevatron; the cross section has been integrated over $66 < Q < 116$ GeV. (b) Comparison of $d\sigma^{\text{fixed}(1)}/dQ_T$ (solid) and $d\sigma^{\text{exp}(1)}/dQ_T$ (dashed) on absolute scale.

3.1. Inverse transforms

When performing the inverse N and b transforms, special attention has to be paid to the singularity in the resummed exponent, Eqs. (15)–(17), at $\beta = 1/2$. For $\eta = 1/4$, the singularity occurs for

$$\chi(\bar{N}, \bar{b}) = \bar{b} + \frac{\bar{N}}{1 + \frac{\bar{b}}{4\bar{N}}} = \exp[1/(2b_0\alpha_s(\mu))] \equiv \rho_L, \quad (36)$$

and is a manifestation of the Landau pole in the strong coupling. The exponent is also ill-defined when $\chi = 0$ and infinity, i.e., at $\bar{b} = -2\bar{N}$ and $\bar{b} = -4\bar{N}$, respectively. We note that the choice $\eta = 1/4$ is made simply to reduce $\chi = 0$ to a linear relation between \bar{b} and \bar{N} . This is not an essential simplification, but it makes the following analysis slightly more convenient. In the following we sketch the application of the method of [10] to this jointly resummed cross section. As far as the Landau pole is concerned, it is simultaneously in the spirit of both the “minimal” prescription proposed for pure threshold resummation in [18], and the “principal value

resummation”, described in [11].

The contour for the inverse Mellin transform is chosen to be bent at an angle ϕ with respect to the real axis and is parameterized as follows (see Fig. 2):

$$N = C + ze^{\pm i\phi} , \quad (37)$$

where the upper (lower) sign applies to the upper (lower) branch of the contour, with $0 \leq z \leq \infty$ ($\infty \geq z \geq 0$). For $\phi > \pi/2$, this results in an exponentially convergent integral over N in the inverse transform, Eq. (2) for all $\tau < 1$ [16, 18]. For the moment, we do not specify the constant C , except that it has to lie to the right of the rightmost singularity of the parton distribution functions. At any finite order in perturbation theory, all values of $C > 0$, and all $\pi > \phi > \pi/2$ are equivalent. In the resummed cross section, however, the singularity at $\chi = \rho_L$ introduces a power-suppressed ambiguity in the transform, which we resolve by choosing $C < \rho_L$ [18].

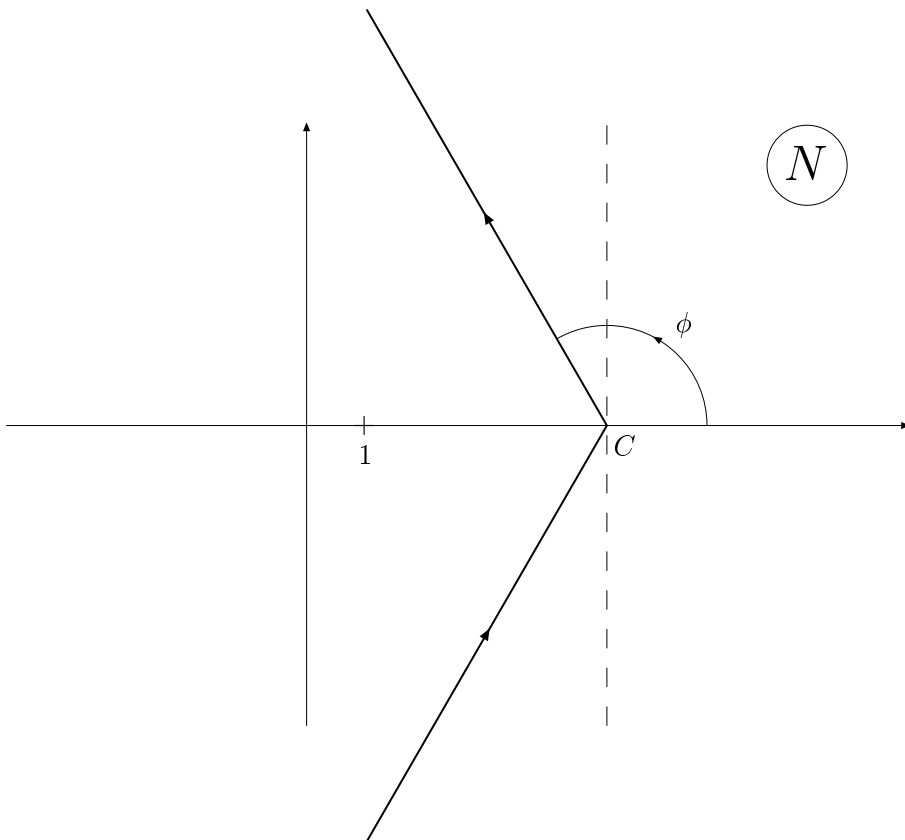


Figure 2: Choice of contour for Mellin inversion.

As mentioned above, the position of the Landau pole depends on both N and b . The d^2b integral in Eq. (2) can be written as

$$\int d^2b e^{i\vec{Q}_T \cdot \vec{b}} f(b) = 2\pi \int_0^\infty db b J_0(bQ_T) f(b) , \quad (38)$$

where J_0 is the Bessel function. Hence, as it stands, the integration over b lies on the positive real axis. This would imply that one would never be able to avoid hitting the Landau pole,

since for any choice of the parameter C in Eq. (37) there is a $b > 0$ for which $\chi(\bar{N}, \bar{b}) = \rho_L$. This problem is of course well-known from standard Q_T resummation. The procedure usually adopted is to prevent b from becoming too large by evaluating the resummed cross section at $b_* = b/\sqrt{1 + b^2/b_{\max}^2}$ [4, 3, 19, 20, 21, 22], at the expense of introducing a new parameter b_{\max} . To avoid introducing a new parameter, we treat the b integral in a manner analogous to the N integral above, avoiding the Landau singularity on a contour that produces an exponentially convergent integral for all $Q_T > 0$.

Were the Landau pole not present we could, instead of performing the b integral along the real axis, use Cauchy's theorem and divert it into complex b space along either of the two solid lines in Fig. 3, under the condition that the integrand falls off sufficiently fast at large $|b|$ and that there be no contribution to the integral at infinitely large real part. To achieve this, we have to split up Eq. (38) as [10]

$$2\pi \int_0^\infty db b J_0(bQ_T) f(b) = \pi \int_0^\infty db b [h_1(bQ_T, v) + h_2(bQ_T, v)] f(b), \quad (39)$$

where we introduce two auxiliary functions $h_{1,2}(z, v)$, related to Hankel functions and defined in terms of an arbitrary real, positive parameter v by integrals in the complex θ -plane [35]:

$$\begin{aligned} h_1(z, v) &\equiv -\frac{1}{\pi} \int_{-iv\pi}^{-\pi+iv\pi} d\theta e^{-iz \sin \theta}, \\ h_2(z, v) &\equiv -\frac{1}{\pi} \int_{\pi+iv\pi}^{-iv\pi} d\theta e^{-iz \sin \theta}. \end{aligned} \quad (40)$$

For h_1 , we parameterize $\theta = -iv\pi + x_\theta\pi(-1 + 2iv)$ ($0 \leq x_\theta \leq 1$), while for h_2 , $\theta = -iv\pi + x_\theta\pi(1 + 2iv)$ ($1 \geq x_\theta \geq 0$). The $h_{1,2}$ become the usual Hankel functions $H_{1,2}(z)$ in the limit $v \rightarrow \infty$. We note that this convergence to the Hankel functions is extremely rapid, since the dependence on the variable v is suppressed by the exponential of an exponential for all finite z . The $h_{1,2}$ are finite for any finite values of z and v . Their sum is always: $h_1(z, v) + h_2(z, v) = 2J_0(z)$, independent of v . The utility of the h -functions is that they distinguish positive and negative phases in Eq. (39), making it possible to treat the b integral as the sum of the two contours in Fig. 3, the one associated with h_1 (h_2) corresponding to closing the contour in the upper (lower) half plane.

The virtue of this technique for the b integration is that we can choose the contours to avoid the Landau pole. We simply need to make sure that the b contour never intersects the trajectories defined by $\chi(\bar{N}, \bar{b}) = \rho_L$, shown by the two light solid curves in Fig. 3. As mentioned earlier, singularities also arise for $\bar{b} = -2\bar{N}$ and $\bar{b} = -4\bar{N}$. These contours are shown in Fig. 3 by the dotted line and the dash-dotted line, respectively. Parameterizing the upper b contour as

$$C_1 : \quad b = \begin{cases} t & (0 \leq t \leq b_c) \\ b_c - te^{-i\phi_b} & (0 \leq t \leq \infty) \end{cases} \quad (41)$$

and the lower one as

$$C_2 : \quad b = \begin{cases} t & (0 \leq t \leq b_c) \\ b_c - te^{i\phi_b} & (0 \leq t \leq \infty) \end{cases}, \quad (42)$$

we choose the parameters b_c and ϕ_b such that none of the branches intersects any of the ‘‘forbidden’’ lines in Fig. 3. A typical choice is also shown in Fig. 3 by the thick solid lines. The parameters C in Eq. (37) and b_c in Eqs. (41), (42) are arbitrary as long as $0 < \left(\frac{C}{1+b_c Q/8C} + \frac{b_c Q}{2}\right) e^{\gamma_E} < \rho_L$.

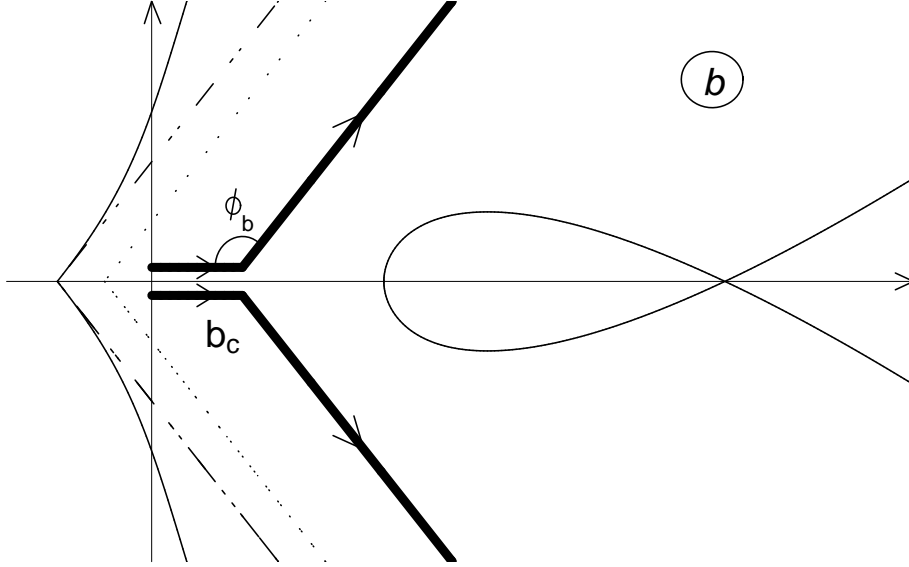


Figure 3: Choice of contour for b integration (thick solid lines). The straight sections of the contour from 0 to b_c are to be interpreted as on the positive real axis. The remaining curves represent lines of singularity discussed in the text.

In this way, our full expression for the cross section in terms of inverse transforms, Eq. (2), becomes

$$\begin{aligned} \frac{d\sigma_{AB}^{\text{res}}}{dQ^2 dQ_T^2} &= \sum_a \sigma_a^{(0)} \int_{C_N} \frac{dN}{2\pi i} \tau^{-N} \left\{ \int_{C_1} \frac{db b}{4\pi} h_1(bQ_T, v) \bar{W}_{AB}^{(a)}(Q, b, N, \mu, \mu_F) \right. \\ &\quad \left. + \int_{C_2} \frac{db b}{4\pi} h_2(bQ_T, v) \bar{W}_{AB}^{(a)}(Q, b, N, \mu, \mu_F) \right\}, \end{aligned} \quad (43)$$

with

$$\begin{aligned} \bar{W}_{AB}^{(a)}(Q, b, N, \mu, \mu_F) &= \exp \left[E_{a\bar{a}}^{\text{PT}}(N, b, Q, \mu) \right] \\ &\quad \times \sum_{j,k} C_{a/j}(N, \alpha_s(\mu)) \mathcal{E}_{jk}(N, Q/\chi, \mu_F) f_{k/A}(N, \mu_F) \\ &\quad \times \sum_{\bar{j}, \bar{k}} C_{\bar{a}/\bar{j}}(N, \alpha_s(\mu)) \mathcal{E}_{\bar{j}\bar{k}}(N, Q/\chi, \mu_F) f_{\bar{k}/B}(N, \mu_F), \end{aligned} \quad (44)$$

for initial hadrons A and B .

This choice of contours in complex transform space is completely equivalent to the original form, Eq. (38) when the exponent is evaluated to finite order in perturbation theory. It is a natural extension of the N -space contour redefinition above [16, 18], using a generalized “minimal” [18] exponent, Eq. (15). As we stressed earlier, joint resummation with its contour integration method provides an alternative to the standard b space resummation. Joint resummation has built-in perturbative treatment of large b values, eliminating the need for a b_* or other prescription for the exponent, or for a freezing of the scale of parton distributions at large b or low Q_T .

To examine the relevance of the large- b contributions, we now compare the jointly resummed Q_T distribution matched to the $\mathcal{O}(\alpha_s)$ perturbative result [2] and the Q_T space resummed [15]

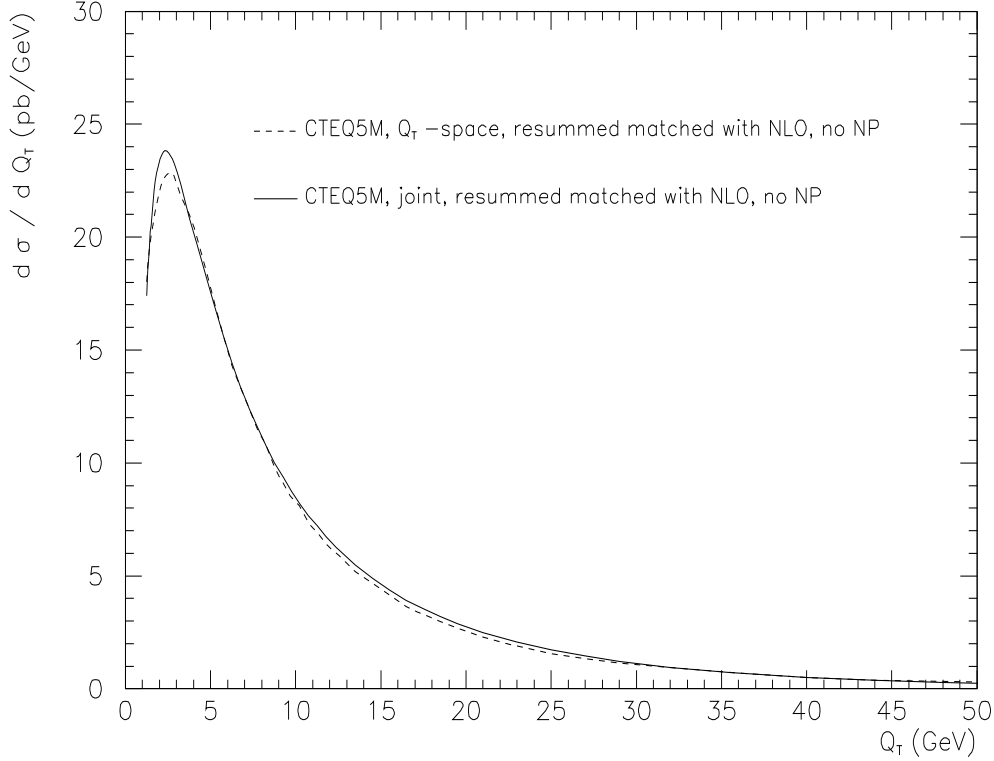


Figure 4: Q_T distribution for Z production at $\sqrt{s} = 1.8$ TeV calculated using the narrow width approximation ($Q = M_Z$). The Q_T space method result and the joint resummation method result are matched to the cross section at $\mathcal{O}(\alpha_s)$. The CTEQ5M [36] parton distributions have been used.

distribution also matched to the $\mathcal{O}(\alpha_s)$ distribution (see the next section for details of the matching procedure). The Q_T space resummation formalism originates from b space resummation and can be viewed as a very good approximation of the latter. Unlike the standard b space technique, direct Q_T resummation, like the contour method just described, yields a result even without any nonperturbative input for nonzero values of Q_T . The two approaches are compared in Fig. 4 for the case of Z boson production at Tevatron energy. As expected, the two distributions differ mostly at the very low- Q_T end of the spectrum.

3.2. Matching to finite order

A resummed Q_T distribution provides theoretical predictions for the small Q_T region; in the large Q_T regime one mainly relies on fixed-order perturbation theory. Thus a description of the intermediate Q_T region requires a consistent matching between the two results that avoids double counting. For the joint resummation we adopt a matching prescription first proposed in standard b space resummation [20]:

$$\frac{d\sigma}{dQ^2 dQ_T^2} = \frac{d\sigma^{\text{res}}}{dQ^2 dQ_T^2} - \frac{d\sigma^{\text{exp(k)}}}{dQ^2 dQ_T^2} + \frac{d\sigma^{\text{fixed(k)}}}{dQ^2 dQ_T^2}, \quad (45)$$

where $d\sigma^{\text{res}}/dQ^2dQ_T^2$ is given in Eq. (2) and, as before, $d\sigma^{\text{exp}(k)}/dQ^2dQ_T^2$ denotes the terms resulting from the expansion of the resummed expression in powers of $\alpha_s(\mu)$ up to the order k at which the fixed-order cross section $d\sigma^{\text{fixed}(k)}/dQ^2dQ_T^2$ is taken (in practice, $k = 1$ (see [2]) or $k = 2$ (see [37])).

Alternatively, one can formulate the matching procedure in the following way [4, 2]:

$$\frac{d\sigma}{dQ^2dQ_T^2} = \frac{d\sigma^{\text{res}}}{dQ^2dQ_T^2} + Y_{\text{finite}} , \quad (46)$$

Y_{finite} standing for the finite part of the fixed-order distribution, i.e. the part remaining after the singular behavior $\propto \alpha_s^k \ln^m(Q^2/Q_T^2)/Q_T^2$, ($2k - 1 \geq m \geq 0$) at k th order of perturbation theory (in our case, $k = 1, 2$) has been taken out of the fixed-order cross section. For pure Q_T resummation, there is no difference between the two ways of matching in Eqs. (45), (46), as long as $d\sigma^{\text{exp}(k)}/dQ^2dQ_T^2$ coincides identically with the singular part of the fixed-order cross section. For our joint resummation, however, $d\sigma^{\text{exp}(k)}/dQ^2dQ_T^2$ also contains terms that are non-singular in Q_T (as in Eq. (23)), which implies that the matching is most naturally performed according to Eq. (45) in conjugate (b, N) space, in order to avoid double counting.

Notably, joint resummation with the choice of $\chi(\bar{N}, \bar{b})$ in Eq. (8) and the matching prescription (45) returns a positive cross section even in the high Q_T regime. This is in contrast to pure Q_T resummation, which notoriously yields a negative answer at large Q_T . To avoid the latter feature, usually an additional switch between the matched cross section and the fixed-order result is implemented in pure Q_T resummation. A nice feature of joint resummation is that this is not necessary here; Eq. (45) is all we need all the way to Q_T of order Q . (Of course, for $Q_T \gg Q$ a further resummation is necessary [38].) The improved large- Q_T behavior of the matched cross section can be traced back to the behavior of the jointly resummed part $d\sigma^{\text{res}}/dQ^2dQ_T^2$ itself, which also remains positive for all values of Q_T . This in turn results from the behavior of the function $\chi(\bar{N}, \bar{b})$ at the small values of b relevant to high Q_T .

A simple argument shows how the small- b behavior of χ ensures that the cross section remains positive at large Q_T for the jointly resummed cross section, and also why it goes negative in pure Q_T resummation in impact parameter space. Consider first pure Q_T resummation, which is equivalent to the choice $\chi = \bar{b}$. For any χ , the one-loop expansion of the resummed exponent in impact parameter space is given by Eq. (22). When $\chi = \bar{b}$ simply ($\bar{N} = 0$ in Eq. (23)), this expression is just as singular at $b = 0$ as for $b \rightarrow \infty$ [39]. This produces a spurious suppression for b small compared to $1/Q$, which is present as well in the full exponent. Because the b integral is dominated by $b \sim 1/Q_T$, this effect is unimportant when Q_T is small. On the other hand, when Q_T is large, of the same order as Q , the suppression of small b removes an important contribution from the b integral. Along the deformed contours of Fig. 3, the situation is particularly simple. Referring to Eq. (43), the sum of the functions $h_1(bQ_T, v)$ and $h_2(bQ_T, v)$ starts out at 2 for $b = 0$, but both begin to oscillate and to decrease exponentially, when $b \sim 1/Q_T$. A spurious suppression times $\bar{W}_{AB}^{(a)}(Q, b, N, \mu, \mu_F)$ for $b \leq 1/Q \sim 1/Q_T$ will thus eliminate positive contributions to the transform, leaving over negative contributions, in the limited range of b in which h_1 and h_2 are themselves of order unity. If, on the other hand, we pick χ as in Eq. (8), then we ensure that the spurious suppression at small b characteristic of pure b -space resummation is absent. The result is a positive cross section for large Q_T .

3.3. Nonperturbative input

In most applications of b space resummation, the perturbative component is supplemented by a Q -dependent Gaussian in impact parameter space, to tune the overall influence of nonperturbative dynamics [4, 19, 20, 21, 22]. Joint resummation implies similar effects in the Q_T distribution at small Q_T . The starting point is the full NLL exponent [9] given in Eq. (3). We expand the Bessel functions in Eq. (3) to derive an explicit form for the leading b - and N -dependence of the resummed exponent, times an integral of the anomalous dimension A_a over soft transverse momenta, defined by a cutoff $\lambda > \Lambda_{\text{QCD}}$,

$$E_{a\bar{a}}^{\text{eik}}(N, b, Q, \mu, \mu_F, \lambda) \sim \left(-\frac{b^2}{2} + \frac{2N^2}{Q^2} \right) \int_0^{\lambda^2} dk_T^2 A_a(\alpha_s(k_T)) \ln \left(\frac{Q}{Nk_T} \right). \quad (47)$$

In this way we derive a standard Gaussian form in b for a multiplicative, nonperturbative smearing function in b space, to account for effects from small k_T . The new feature here is that the coefficient of b^2 is essentially identical to that of the threshold-related power correction $(N/Q)^2$. In our numerical applications below, we will be rather far away from threshold, and as a result we will be mainly sensitive to moderately small N . Hence we will retain only the term $\sim b^2$ in Eq. (47). Thus our nonperturbative smearing function reverts to the purely Gaussian one usually used in Q_T resummation, and we will make the following replacement in the resummed cross section:

$$E_{a\bar{a}}^{\text{PT}}(N, b, Q, \mu) \longrightarrow E_{a\bar{a}}^{\text{PT}}(N, b, Q, \mu) - gb^2, \quad (48)$$

where g is a parameter to be determined by comparison to data. Note that Eq. (47) implies that, as usual, g has a component that depends logarithmically on Q [4, 19, 20, 21, 22, 40].

4. Vector boson production in the framework of joint resummation

With the developments discussed above, the joint resummation formalism becomes a practical tool for the description of electroweak annihilation. Here we consider Z boson production at the Tevatron collider. Recent data on the Q_T distribution of the produced Z bosons are available from both CDF [41] and D0 [42] experiments and have reached a good level of precision. The overall normalization of the data will be treated as a free parameter in our analysis, and will be varied within the quoted experimental errors.

All results are obtained using CTEQ5M parton distribution functions [36], in the manner described in Appendix B. We choose the factorization and renormalization scales $\mu = \mu_F = Q$. The numerical values of the electroweak parameters we use are as follows: $M_Z = 91.187$ GeV, $\sin^2 \theta_W = 0.224$, $\Gamma_Z = 2.49$ GeV. Note that the experimental data sets have been integrated over finite regions in Q , $66 < Q < 116$ GeV for CDF and $75 < Q < 105$ GeV for D0. The inverse transforms are performed as described in Section 3.1., with the following choice of the contour parameters in Figs. 1 and 2: $\phi = \phi_b = 25/32 \pi$, $C = 1.3$, $b_c = 0.2/Q$. Of course we are free to choose these parameters differently, as long as they are such that the structure of the contours as depicted in Fig. 3 is maintained. Finally, as mentioned above, we choose $\eta = 1/4$ in Eq. (8). We have checked that the result is quite insensitive to this choice, at the order of a percent when η is changed by a factor of 2 at $Q_T = 4$ GeV.

As we pointed out before, an attractive feature of the joint resummation with transforms defined as above is that we can obtain predictions that have no dependence on any additional nonperturbative parameter. Results of this form are shown by the dashed lines in Figs. 5 and 6. In both cases, we have adjusted the normalization of the theory curve so that the χ^2 of the comparison between data and theory becomes minimal. For the CDF data, this normalization factor is 1.035, for D0 it is 0.96. It is evident from Figs. 5 and 6 that our “purely perturbative” predictions correctly reproduce the trend of the data over most of the measured region in Q_T , but peak at too small Q_T . This is no surprise of course, since we expect nonperturbative effects to play a non-negligible role at low Q_T . For comparison, Fig. 5 also displays the fixed-order ($\mathcal{O}(\alpha_s)$, dotted lines, and $\mathcal{O}(\alpha_s^2)$, dash-dotted lines ¹) results for the cross section, with their well-known divergent behavior at small Q_T .

Interestingly, the fixed-order $\mathcal{O}(\alpha_s)$ result misses the data also at *large* Q_T , where it remains too low even if the normalization is adjusted within the errors quoted in experiment. Joint resummation, with the choice Eq. (8) for $\chi(\bar{N}, \bar{b})$ and the matching procedure described in Eq. (45), adds an important contribution to the cross section also here: the difference $d\sigma^{\text{res}}/dQ^2dQ_T^2 - d\sigma^{\text{exp}(1)}/dQ^2dQ_T^2$ in Eq. (45) remains numerically significant also at large Q_T and appears to be crucial for bringing the theoretical calculation to the data. As can be seen from Fig. 5, the cross section at $\mathcal{O}(\alpha_s^2)$, $d\sigma^{\text{fixed}(2)}/dQ^2dQ_T^2$, is larger than $d\sigma^{\text{fixed}(1)}/dQ^2dQ_T^2$. As expected, the difference $d\sigma^{\text{res}}/dQ^2dQ_T^2 - d\sigma^{\text{exp}(2)}/dQ^2dQ_T^2$ is *smaller* than $d\sigma^{\text{res}}/dQ^2dQ_T^2 - d\sigma^{\text{exp}(1)}/dQ^2dQ_T^2$, so that the full cross section in Eq. (45) depends only little on whether matching is performed at $\mathcal{O}(\alpha_s)$ or at $\mathcal{O}(\alpha_s^2)$. We take this feature as an indication that our approach for matching, Eq. (45), is justified and reasonable even at large $Q_T \sim Q$.

To improve the low- Q_T behavior further, we introduce a nonperturbative function as described in Eq. (48). Since most of the cross section comes from the region $Q \sim M_Z$, we neglect the mild (logarithmic) dependence of the nonperturbative parameter g on Q . We then fit g to the CDF and D0 data simultaneously, allowing again the normalizations to vary for the two data sets. Since g should be determined from the low- Q_T region, we include only the data points with $Q_T < 50$ GeV in this fit. The results of the fit do, however, not depend much on this choice. The optimal result is obtained for $g = 0.8$ GeV² and the normalization factors 1.069 (0.975) for CDF (D0). The χ^2 for the 42 (20) data points from CDF (D0) included in the fit is 31.3 (23.4). Even better fits would be possible by using a more refined nonperturbative function, as suggested by Eq. (47), resulting in extra parameters. As can be seen from the solid lines in Figs. 5 and 6, with these parameters a very good agreement between the jointly resummed cross section, matched with the fixed-order cross section at $\mathcal{O}(\alpha_s)$, and the data is achieved. We note that our nonperturbative parameter $g = 0.8$ GeV² is very similar to that determined in Ref. [23], where an extrapolation of the perturbation theory result to large b was made. Ref. [23] argued that the b integral in pure- Q_T resummation is dominated by the saddle point. Our method and theirs lead to somewhat smaller values of the nonperturbative parameter than when a b_* prescription is used [21].

5. Conclusions

The transverse momentum distribution of the Z is by now a well-studied problem, to which a number of successful analyses have been applied [14, 15, 21, 22, 23]. We have come back to

¹We have used subroutines of the RESBOS package of Ref. [22] in order to calculate the cross section at $\mathcal{O}(\alpha_s^2)$.

this topic because we believe that the method of joint resummation offers additional insight on the interplay of perturbative and nonperturbative corrections in this, and other hadronic reactions. Joint resummation, implemented as above, provides a convenient definition of the perturbative cross section at any nonzero Q_T , without the introduction of additional dimensional scales (beyond Λ_{QCD}) to define either the perturbative resummation or the parton distributions at low scales.

Treated this way, the jointly resummed cross section retains its original perturbative asymptotic expansion order by order. It also suggests the functional form of nonperturbative corrections. Because perturbative and nonperturbative components of a QCD cross section are linked at the level of power corrections [11, 12], it will be necessary, and useful, to reanalyze the functional and phenomenological aspects of nonperturbative corrections in this formalism, relying on the available range of data for the Drell-Yan mechanism. Toward the high-energy side, a further application to Higgs production [28, 43] at the LHC will also be of interest. In the same spirit, we intend as well to return to the application of joint resummation to semi-inclusive processes such direct photon production [9, 10].

Acknowledgments

We are grateful to A. Vogt for valuable discussions on Ref. [31], and for providing a version of his code for the NLO evolution of parton densities in which the iterative procedures for approximating the ordered exponentials are implemented. We are also thankful to C. Balazs, P. Nadolsky and C.P. Yuan for helpful communications on the use of the RESBOS code [22], and we thank D. de Florian, E. Laenen and J.-W. Qiu for useful discussions. The work of G.S. was supported in part by the National Science Foundation, grants PHY9722101 and PHY0098527. W.V. is grateful to RIKEN, Brookhaven National Laboratory and the U.S. Department of Energy (contract number DE-AC02-98CH10886) for providing the facilities essential for the completion of this work. A.K. thanks the U.S. Department of Energy (contract number DE-AC02-98CH10886) for support.

A Some useful formulas

For Z boson production one has in Eq. (2) the standard tree-level cross sections (see [44]):

$$\begin{aligned}
\sigma_a^{(0)} &= \frac{4\pi^2\alpha^2}{9\tau S^2} \hat{e}_a^2 \\
\hat{e}_a^2 &= e_a^2 - 2e_a v_l v_a \kappa \frac{Q^2(Q^2 - M_Z^2)}{(Q^2 - M_Z^2)^2 + M_Z^2 \Gamma_Z^2} \\
&\quad + (a_l^2 + v_l^2)(a_a^2 + v_a^2) \kappa^2 \frac{Q^4}{(Q^2 - M_Z^2)^2 + M_Z^2 \Gamma_Z^2} \\
\kappa &= \frac{\sqrt{2}G_F M_Z^2}{4\pi\alpha} \\
a_l &= -\frac{1}{2} \quad , \quad v_l = -\frac{1}{2} + 2\sin^2\theta_W \quad , \\
a_a &= T_a^3 \quad , \quad v_a = T_a^3 - 2e_a \sin^2\theta_W \quad .
\end{aligned} \tag{49}$$

B Using x -space parton distributions

The above formulas are directly applicable if the parton densities, including their evolution, are treated in Mellin moment space. In this context, it is convenient to use the evolution code of [32] which is set up in moment space. In practical applications, however, one may prefer to be more flexible concerning the choice of parton densities and be able to make direct use of any (x -space) parameterization on the market [36, 45]. One way of achieving this was presented in Ref. [18]. Here we propose a new simple method. Let us first rewrite Eqs. (2), (25) as

$$\frac{d\sigma^{\text{res}}}{dQ^2 dQ_T^2} = \frac{1}{2\pi i} \int_{C_N} dN \tau^{-N} \sum_{i,j} f_{i/H}(N, \mu_F) f_{j/H}(N, \mu_F) \hat{\sigma}_{ij}^{\text{res}}(N, Q, Q_T, \mu, \mu_F), \quad (50)$$

which is obtained after performing the d^2b integration in Eq. (2). The $\hat{\sigma}_{ij}^{\text{res}}$ are then resummed partonic cross sections, differential in Q_T .

The inverse-moment expression in Eq. (50) is of course identical to an x -space convolution of the parton densities with the resummed cross section :

$$\frac{d\sigma^{\text{res}}}{dQ^2 dQ_T^2} \equiv \sum_{i,j} \int_{\tau}^{\infty} \frac{dz}{z} \int_{\tau/z}^1 \frac{dy}{y} \tilde{f}_i(y, \mu_F) \tilde{f}_j\left(\frac{\tau}{yz}, \mu_F\right) \tilde{\sigma}_{ij}^{\text{res}}(z, Q, Q_T, \mu, \mu_F), \quad (51)$$

where $z = Q^2/\hat{s}$, the $\tilde{f}_i(x, \mu_F)$ are the x -space parton densities, and $\tilde{\sigma}_{ij}^{\text{res}}(z, Q, Q_T, \mu, \mu_F)$ is given by the inverse Mellin transform of the moments $\hat{\sigma}_{ij}^{\text{res}}(N, Q, Q_T, \mu, \mu_F)$,

$$\tilde{\sigma}_{ij}^{\text{res}}(z, Q, Q_T, \mu, \mu_F) = \frac{1}{2\pi i} \int_{C_N} dN z^{-N} \hat{\sigma}_{ij}^{\text{res}}(N, Q, Q_T, \mu, \mu_F). \quad (52)$$

As was pointed out in [18], and as is indicated by the upper limit ∞ in Eq. (51), the function $\tilde{\sigma}_{ij}^{\text{res}}(z, Q, Q_T, \mu, \mu_F)$ defined in the “minimal” prescription is non-vanishing also at $z > 1$ due to the presence of the Landau pole to the right of the N space contour (see Fig. 2), even though it rapidly decreases with increasing z . At $z > 1$, the angle ϕ of the N -space contour has to be decreased to below $\pi/2$ to obtain a convergent result.

The right-hand side of Eq. (51) in principle allows for using x -space parton distributions. However, a problem arises from the fact that the resummed cross section is highly singular [16] at $z \rightarrow 1$ (even though regularized in terms of plus-distributions), which makes the convolution with the parton densities numerically very tedious [18]. A convenient way of eliminating this problem is to trivially rewrite Eq. (50) as

$$\frac{d\sigma^{\text{res}}}{dQ^2 dQ_T^2} = \frac{1}{2\pi i} \int_{C_N} dN \tau^{-N} \sum_{i,j} [(N-1) f_{i/H}(N, \mu_F)] [(N-1) f_{j/H}(N, \mu_F)] \frac{\hat{\sigma}_{ij}^{\text{res}}(N, Q, Q_T, \mu, \mu_F)}{(N-1)^2}. \quad (53)$$

The Mellin-inverse of $\hat{\sigma}_{ij}^{\text{res}}(N, Q, Q_T, \mu, \mu_F)/(N-1)^2$,

$$\mathcal{S}_{ij}^{\text{res}}(z, Q, Q_T, \mu, \mu_F) = \frac{1}{2\pi i} \int_{C_N} dN z^{-N} \frac{\hat{\sigma}_{ij}^{\text{res}}(N, Q, Q_T, \mu, \mu_F)}{(N-1)^2}, \quad (54)$$

is now sufficiently well-behaved at large z thanks to the extra suppression by $1/(N-1)^2$. For the inverse of $(N-1) f_{i/H}(N, \mu_F)$ one finds, making use of the fact that the x -space parton densities vanish at $x = 1$:

$$\frac{1}{2\pi i} \int_{C_N} dN x^{-N} (N-1) f_{i/H}(N, \mu_F) = -\frac{d}{dx} [x \tilde{f}_i(x, \mu_F)] \equiv \mathcal{F}(x, \mu_F). \quad (55)$$

We thus arrive at

$$\frac{d\sigma^{\text{res}}}{dQ^2 dQ_T^2} \equiv \sum_{i,j} \int_{\tau}^{\infty} \frac{dz}{z} \int_{\tau/z}^1 \frac{dy}{y} \mathcal{F}_i(y, \mu_F) \mathcal{F}_j\left(\frac{\tau}{yz}, \mu_F\right) \mathcal{S}_{ij}^{\text{res}}(z, Q, Q_T, \mu, \mu_F), \quad (56)$$

which has good numerical behavior. The standard sets [32, 36, 45] of the parton distributions allow taking the first derivative numerically. Depending on the large- N behavior of the resummed cross section in moment space, $\hat{\sigma}_{ij}^{\text{res}}(N, Q, Q_T, \mu, \mu_F)$, it may be necessary to divide by a higher power of $N - 1$ in Eq. (54), resulting in higher derivatives of the parton distributions in Eq. (55). This turns out to be the case for the gluon-gluon initial state in inclusive Higgs production via $gg \rightarrow HX$ [46].

References

- [1] Yu.L. Dokshitzer, D.I. D’Yakonov, and S.I. Troyan, Phys. Lett. **79B** (1978) 269; G. Parisi and R. Petronzio, Nucl. Phys. **B154** (1979) 427.
- [2] G. Altarelli, R.K. Ellis, M. Greco and G. Martinelli, Nucl. Phys. **B246** (1984) 12.
- [3] J.C. Collins and D.E. Soper, Nucl. Phys. **B193** (1981) 381; E: **B213** (1983) 545; Nucl. Phys. **B197** (1982) 446.
- [4] J.C. Collins, D.E. Soper and G. Sterman, Nucl. Phys. **B250** (1985) 199.
- [5] G. Sterman, Nucl. Phys. **B281** (1987) 310.
- [6] S. Catani and L. Trentadue, Nucl. Phys. **B327** (1989) 323, **B353** (1991) 183.
- [7] E.L. Berger and H. Contopanagos, Phys. Rev. D57 (1998) 253; R. Bonciani, S. Catani, M.L. Mangano and P. Nason Nucl. Phys. **B529** (1998) 424, hep-ph/9801375; N. Kidonakis and R. Vogt Phys. Rev. D59 (1999) 074014, hep-ph/9806526; S. Catani, M.L. Mangano, P. Nason, C. Oleari and W. Vogelsang, JHEP 9903 (1999) 025, hep-ph/9903436; G. Sterman and W. Vogelsang, proceedings of the “International Europhysics Conference on High-Energy Physics (EPS-HEP 99)”, Tampere, Finland, July 1999, eds. K. Huitu, H. Kurki-Suonio, J. Maalampi, p.423, hep-ph/9910371; N. Kidonakis and J.F Owens, Phys. Rev. D61 (2000) 094004, hep-ph/9912388; G. Sterman and W. Vogelsang, JHEP 0102 (2001) 016, hep-ph/0011289.
- [8] H.-N. Li, Phys. Lett. **B454** (1999) 328, hep-ph/9812363.
- [9] E. Laenen, G. Sterman, and W. Vogelsang, Phys. Rev. **D63** (2001) 114018, hep-ph/0010080.
- [10] E. Laenen, G. Sterman, and W. Vogelsang, Phys. Rev. Lett. **84** (2000) 4296, hep-ph/0002078.
- [11] H. Contopanagos and G. Sterman, Nucl. Phys. **B419** (1994) 77, hep-ph/9310313.

- [12] B.R. Webber, Phys. Lett. **B339** (1994) 148, hep-ph/9408222; G.P. Korchemsky, G. Sterman, Nucl. Phys. **B437** (1995) 415, hep-ph/9411211; and in *Proc. of the XXX Rencontres de Moriond: QCD and High Energy Hadronic Interactions*, ed. J. Trân Thanh Vân, Editions Frontiers, (Paris, 1995), p. 383; hep-ph/9505391; Yu.L. Dokshitzer, B.R. Webber, Phys. Lett. **B352** (1995) 451, hep-ph/9504219; R. Akhoury, V.I. Zakharov, Nucl. Phys. **B465** (1996) 295, hep-ph/9507253; see also: M. Beneke, Phys. Rept. **317** (1999) 1, and references therein.
- [13] N. Kidonakis and J.F. Owens, Phys. Rev. **D63** (2001) 054019, hep-ph/0007268; N. Kidonakis, E. Laenen, S. Moch and R. Vogt, Phys. Rev. **D64** (2001) 114001, hep-ph/0105041.
- [14] R.K. Ellis and S. Veseli, Nucl. Phys. **B511** (1998) 649, hep-ph/9706526.
- [15] A. Kulesza and W.J. Stirling, Nucl. Phys. **B555** (1999) 279, hep-ph/9902234; Eur. Phys. J. **C20** (2001) 349, hep-ph/0103089.
- [16] H. Contopanagos and G. Sterman, Nucl. Phys. **B400** (1993) 211.
- [17] E.L. Berger and H. Contopanagos, Phys. Rev. **D57** (1998) 253, hep-ph/9706206.
- [18] S. Catani, M.L. Mangano, P. Nason and L. Trentadue, Nucl. Phys. **B478** (1996) 273, hep-ph/9604351.
- [19] C. Davies and W.J. Stirling, Nucl. Phys. **B244** (1984) 337; C. Davies, W.J. Stirling and B.R. Webber, Nucl. Phys. **B256** (1985) 413.
- [20] P.B. Arnold and R.P. Kauffman, Nucl. Phys. **B349** (1991) 381.
- [21] G.A. Ladinsky and C.-P. Yuan, Phys. Rev. **D50** (1994) 4239 hep-ph/9311341; F. Landry, R. Brock, G. Ladinsky and C.P. Yuan, Phys. Rev. **D63** (2001) 013004, hep-ph/9905391.
- [22] C. Balazs and C.P. Yuan, Phys. Rev. **D56** (1997) 5558, hep-ph/9704258.
- [23] J.-W. Qiu and X.-F. Zhang Phys. Rev. Lett. **86** (2001) 2724, hep-ph/0012058; Phys. Rev. **D63** (2001) 114011, hep-ph/0012348.
- [24] N. Kidonakis, Phys. Rev. **D64** (2001) 014009, hep-ph/0010002.
- [25] J. Kodaira and L. Trentadue, Phys. Lett. **B112** (1982) 66; *ibid.* **B123** (1983) 335; S. Catani, E. D’Emilio and L. Trentadue, Phys. Lett. **B211** (1988) 335.
- [26] S. Catani and L. Trentadue, Nucl. Phys. **B327** (1989) 323; *ibid.* **B353** (1991) 183.
- [27] D. de Florian and M. Grazzini, Phys. Rev. Lett. **85** (2000) 4678, hep-ph/0008152; Nucl. Phys. **B616** (2001) 247, hep-ph/0108273.
- [28] S. Catani, D. de Florian and M. Grazzini, Nucl. Phys. **B596** (2001) 299, hep-ph/0008184.

- [29] G. Altarelli and G. Parisi, Nucl. Phys. **B126** (1977) 298; Yu. L. Dokshitzer, Sov. Phys. JETP **46** (1977) 641; L. N. Lipatov, Sov. J. Nucl. Phys. **20** (1975) 95; V.N. Gribov and L.N. Lipatov, Sov. J. Nucl. Phys. **15** (1972) 438; M. Ahmed and G. Ross, Phys. Lett. **B56** (1975) 385; Nucl. Phys. **B111** (1976) 298; E.G. Floratos, D.A. Ross and C.T. Sachrajda, Nucl. Phys. **B129** (1977) 66; E: **B139** (1978) 545 ; Nucl. Phys. **B152** (1979) 493; A. Gonzales-Arroyo, C. Lopez and F.J. Yndurain, Nucl. Phys. **B153** (1979) 161; A. Gonzales-Arroyo and C. Lopez, Nucl. Phys. **B166** (1980) 429; E.G. Floratos, C. Kounnas and R. Lacaze, Phys. Lett. **98B** (1981) 89,285; Nucl. Phys. **B192** (1981) 417; G. Curci, W. Furmanski and R. Petronzio, Nucl. Phys. **B175** (1980) 27; W. Furmanski and R. Petronzio, Phys. Lett. **97B** (1980) 437.
- [30] W. Furmanski and R. Petronzio, Z. Phys. **C11** (1982) 293.
- [31] J. Blümlein and A. Vogt, Phys. Rev. **D58** (1998) 014020.
- [32] M. Glück, E. Reya and A. Vogt, Eur. Phys. J. **C5** (1998) 461, hep-ph/9806404.
- [33] O. Martin, A. Schäfer, M. Stratmann and W. Vogelsang, Phys. Rev. **D60** (1999) 117502, hep-ph/9902250.
- [34] S. Catani, D. de Florian and M. Grazzini, JHEP **0105** (2001) 025, hep-ph/0102227; see also: M. Krämer, E. Laenen and M. Spira, Nucl. Phys. **B511** (1998) 523, R.V. Harlander and W.B. Kilgore, Phys. Rev. **D64** (2001) 013015, hep-ph/0102241.
- [35] I.S. Gradshteyn and I.M. Ryzhik, *Table of Integrals, Series, and Products*, Academic Press, San Diego, 1979, p.957.
- [36] CTEQ Collab., H.-L. Lai *et al.*, Eur. Phys. J. **C12** (2000) 375, hep-ph/9903282.
- [37] R.K. Ellis, G. Martinelli and R. Petronzio, Phys. Lett. **B104** (1981) 45; Nucl. Phys. **B211** (1983) 106; P. Arnold and M.H. Reno, Nucl. Phys. **B319** (1989) 37, E: **B330** (1990) 284; P. Arnold, R.K. Ellis and M.H. Reno, Phys. Rev. **D40** (1989) 912; R.J. Gonsalves, J. Pawlowski, C.f. Wai, Phys. Rev. **D40** (1989) 2245; Phys. Lett. **B252** (1990) 663.
- [38] E.L. Berger, J.-W. Qiu and X.-F. Zhang, hep-ph/0107309.
- [39] S. Frixione, P. Nason and G. Ridolfi, Nucl. Phys. **B542** (1999) 311, hep-ph/9809367.
- [40] S. Tafat, JHEP **0105**, (2001) 004; hep-ph/0102237.
- [41] CDF Collab., T. Affolder *et al.*, Phys. Rev. Lett. **84** (2000) 845.
- [42] D0 Collab., B. Abbott *et al.*, Phys. Rev. **D61** (2000) 032004; Phys. Rev. Lett. **84** (2000) 2792.
- [43] C. Balazs and C.P. Yuan, Phys. Lett. **B478** (2000) 192, hep-ph/0001103.
- [44] Particle Data Group, D.E. Groom *et al.*, Eur. Phys. J. **C15** (2000) 1.

- [45] A.D. Martin, R.G. Roberts, W.J. Stirling, R.S. Thorne, Eur. Phys. J. **C14** (2000) 133, hep-ph/990723; hep-ph/0106075.
- [46] A. Kulesza, G. Sterman and W. Vogelsang, in preparation.

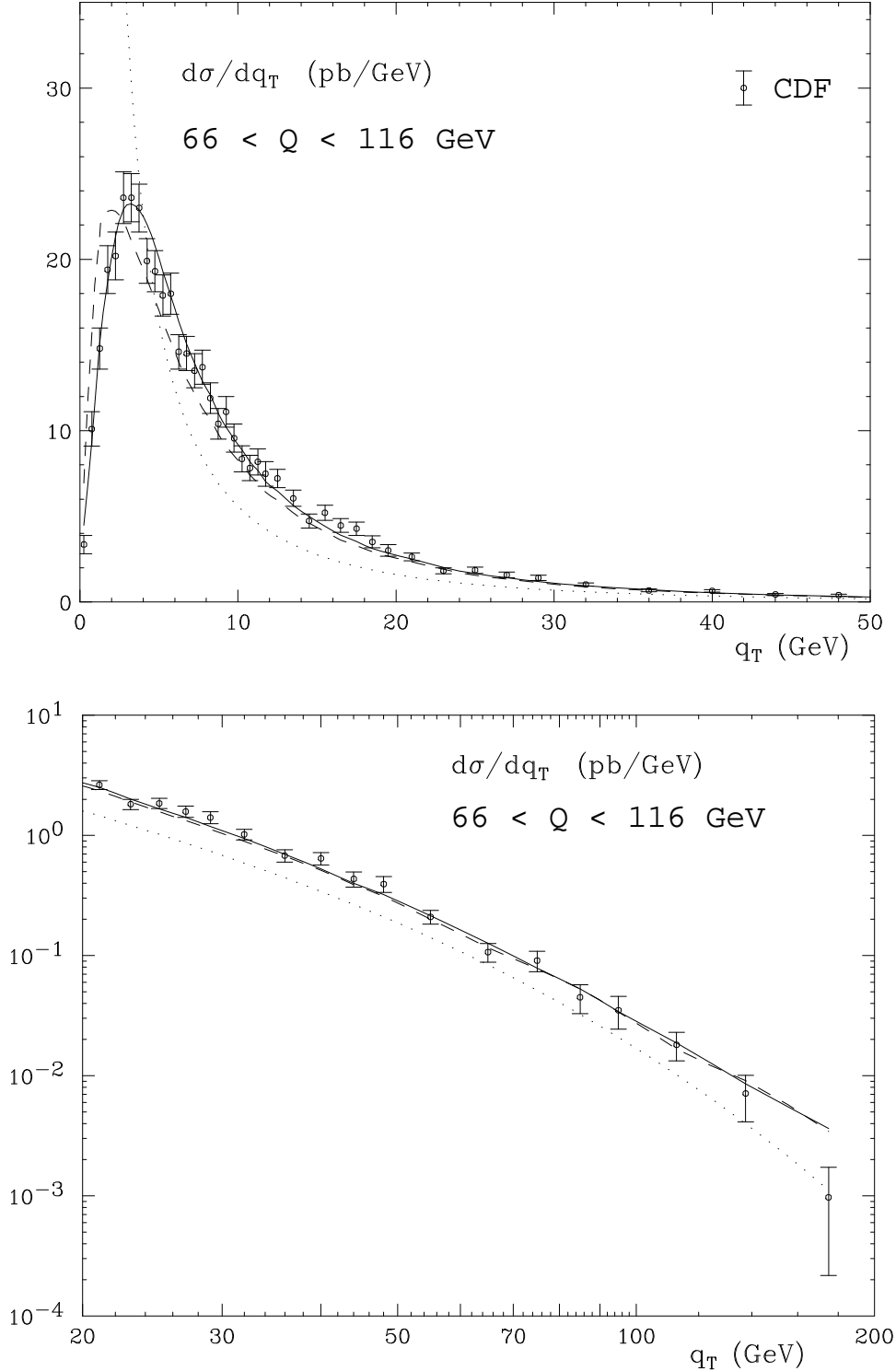


Figure 5: CDF data [41] on Z production compared to joint resummation predictions (matched to the $\mathcal{O}(\alpha_s)$ result according to Eq. (45)) without nonperturbative smearing (dashed) and with Gaussian smearing using the nonperturbative parameter $g = 0.8 \text{ GeV}^2$ (solid). The normalizations of the curves have been adjusted in order to give an optimal description; see text. The dotted and dash-dotted lines show the fixed-order results at $\mathcal{O}(\alpha_s)$ and $\mathcal{O}(\alpha_s^2)$, respectively. The lower plot makes the large Q_T region more visible.

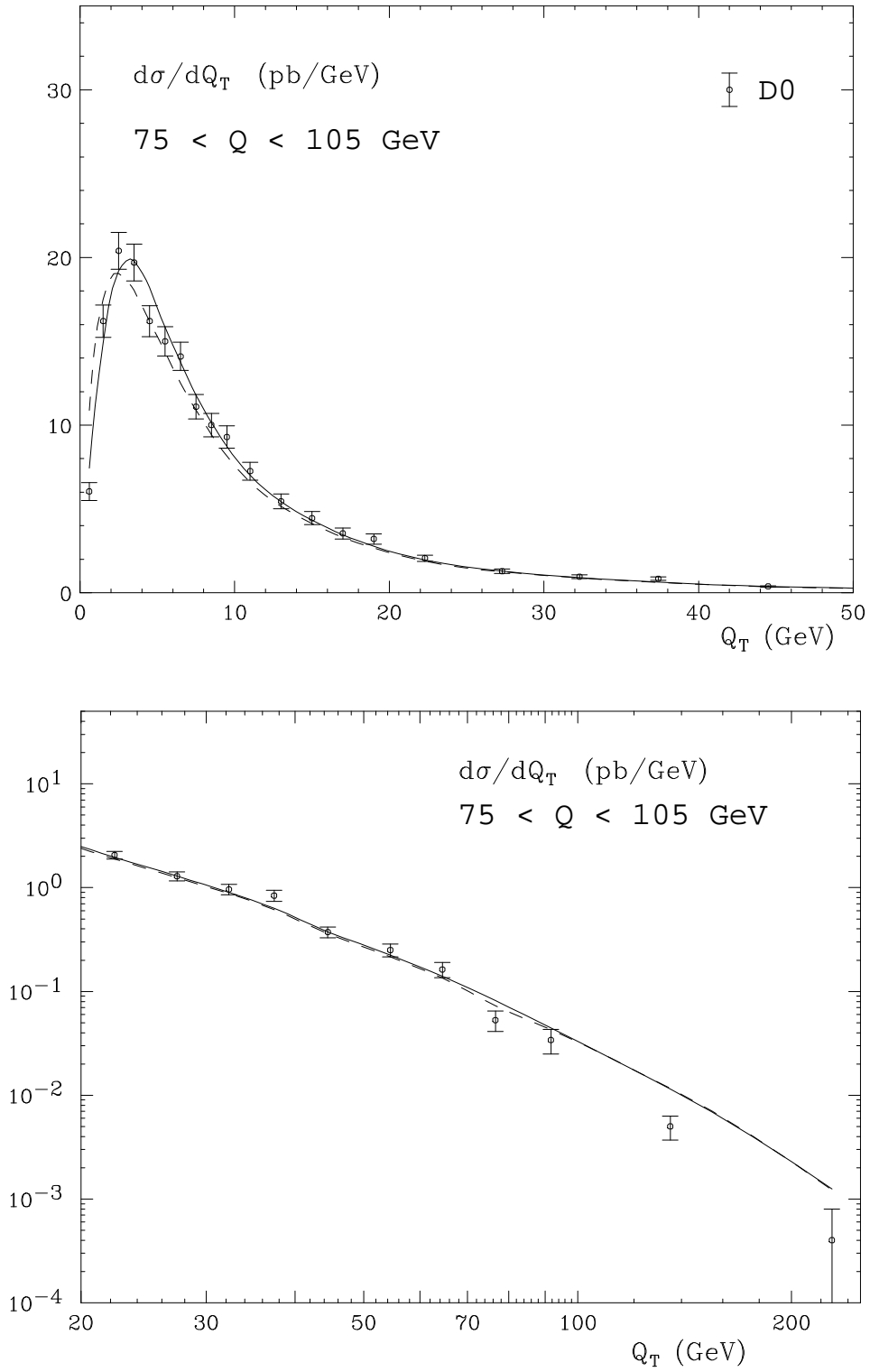


Figure 6: Same as Fig. 5, but compared to the D0 data [42].